Beyond the 2023 surge: Quantifying shoreline dynamics in the German Baltic Sea with Sentinel-2

Eike M. Schütt[1], Kerstin Stelzer[2], Jorrit Scholze[2], Marcel König[2], Lutz Christiansen[3] and Natascha Oppelt[4]

[1] *Earth Observation and Modelling, Department of Geography, Kiel University, Kiel, Germany schuett@geographie.uni-kiel.de*
[2] *Brockmann Consult GmbH, Hamburg, Germany*
[3] *Schleswig-Holstein Agency for Coastal Defence, National Park and Marine Conservation (LKN.SH), Husum, Germany*
[4] *Earth Observation and Modelling, Department of Geography, Kiel University, Kiel, Germany*

Summary

Monitoring coastal zones is essential for evidence-based coastal management. Commonly applied methods and technologies like beach surveys, aerial imagery, and Light Detection and Ranging (LiDAR) provide highly accurate data but are often limited in spatial coverage or monitoring frequency due to high costs. Satellite remote sensing has emerged as a promising and cost-effective alternative, offering frequent, large-scale shoreline observations. To facilitate rapid and precise satellite-based shoreline change analysis across large regions, we developed the Shoreline Extraction and Change Analysis Tool (SEaCAT). This Python-based toolkit leverages cloud technology to semi-automate key stages of data processing, including scene selection, shoreline extraction, and change analysis. We employ SEaCAT to assess the impact of the October 2023 storm surge on coastal morphology in two regions along the German Baltic Sea coast. By analysing the entire Sentinel-2 archive (July 2015 to June 2024), we contextualize the event within broader morphodynamic trends and observe post-storm recovery. Our findings reveal that due to differences in the surges' duration and intensity, it had a significantly higher morphodynamic impact in Angeln, Schleswig-Holstein, compared to Mönchgut, Mecklenburg-Vorpommern. Despite this, recovery processes in the months after the surge mitigated the surge's effects along most coastal sections. However, the Schleimünde sand spit emerges as an erosion hotspot, experiencing continued coastal recession for approximately six months post-surge due to a dramatically altered spit profile. Our study demonstrates that, although satellite-based shoreline monitoring may not achieve the accuracy of commonly employed methods, its frequent observations and low costs make it a valuable complement to existing monitoring strategies.

Keywords

shoreline monitoring, satellite derived shoreline, shoreline change analysis, Sentinel-2, storm surge, extreme event, erosion, coastal morphodynamics

Received 30.09.2024, reviewed 21.10.2024, revised 09.12.2024, accepted 23.12.2024, available online 04.02.2025.

Zusammenfassung

Das Monitoring von Küstenzonen ist eine wesentliche Grundlage für ein evidenzbasiertes Küstenmanagement. Gängige Methoden wie GPS-Vermessungen oder die Auswertung von Luftbildern oder Laserscans liefern zwar hochpräzise Daten, sind jedoch häufig aufgrund hoher Kosten in der räumlichen Abdeckung oder der Vermessungshäufigkeit eingeschränkt. Um diese Datenlücken zu schließen, bietet sich die Satellitenfernerkundung als vielversprechende und kostengünstige Methode an, die regelmäßige, großflächige Beobachtungen der Küstenlinie ermöglicht. Um eine schnelle und präzise satellitengestützte Analyse von Küstenlinienveränderungen über große Regionen hinweg zu erleichtern, haben wir das 'Shoreline Extraction and Change Analysis Tool' (SEaCAT) entwickelt. Dieses Python-basierte Toolkit nutzt Cloud-Technologie, um zentrale Schritte der Datenverarbeitung, wie die Szenenauswahl, Küstenlinienextraktion und Veränderungsanalyse größtenteils zu automatisieren. Mithilfe von SEaCAT zeigen wir die Auswirkungen der Sturmflut vom Oktober 2023 auf die Küstenmorphologie in zwei Regionen der deutschen Ostseeküste. Durch die Analyse des gesamten Sentinel-2-Archivs (Juli 2015 bis Juni 2024) setzen wir die Sturmflut in einen morphodynamischen Kontext und beobachten Veränderungen nach dem Sturm. Unsere Ergebnisse zeigen, dass die Sturmflut aufgrund längerer Dauer und höherer Intensität einen deutlich stärkeren morphodynamischen Einfluss in Angeln, Schleswig-Holstein, als im Mönchgut, Mecklenburg-Vorpommern, hatte. Durch natürliche Ausgleichsprozesse in den Monaten nach der Sturmflut wurden ihre Auswirkungen auf die Küstenlinie in vielen Regionen abgemildert. Eine Ausnahme bildet der Nehrungshaken von Schleimünde, der aufgrund eines stark veränderten Höhenprofils bis etwa sechs Monate nach der Sturmflut einen Küstenrückgang verzeichnete. Mithilfe dieser Studie demonstrieren wir, dass satellitengestütztes Küstenlinienmonitoring zwar nicht die gleiche Genauigkeit herkömmlicher Methoden erreicht, durch kurze Aufnahmeintervalle und geringe Kosten aber trotzdem eine wertvolle Ergänzung zu bisher eingesetzten Methoden zum Küstenmonitoring darstellt.

Schlagwörter

Küstenmonitoring, Küstenlinie, Uferlinie, Satellit, Sentinel-2, Sturmflut, Erosion, Morphodynamik, Veränderungsanalyse

1 Introduction

Shorelines are the dynamic boundary between land and sea. Wind, waves and currents constantly change shoreline morphology through erosion and accumulation of sediments (Wright and Short 1984, Weisse et al. 2021, Castelle and Masselink 2023). Extreme events, such as storm surges, significantly accelerate morphological evolution and may lead to abrupt shoreline changes (Łabuz and Kowalewska-Kalkowska 2011, Harley et al. 2017). With the expected increase in extreme events due to climate change and the dynamic, non-linear response of coastal morphology to sea level rise, morphological evolution will expedite further (Łabuz 2015, Passeri et al. 2015, Vousdoukas et al. 2020, Meier et al. 2022, Pang et al. 2023).

As shoreline dynamics continue to evolve, morphological changes pose increasing risks to communities, assets, and infrastructure in the coastal zone. These hazards include flooding, property damage and loss of land through erosion (Nicholls and Cazenave 2010, Hallegatte et al. 2013). Addressing these threats requires a comprehensive understanding

of coastal processes and an effective coastal management (Jacobson et al. 2014, Williams et al. 2018).

Coastal management critically depends on accurate and frequent monitoring data to identify morphodynamic hotspots and evaluate the effectiveness of coastal protection measures (Pikelj et al. 2018, Williams et al. 2018), but existing monitoring schemes are limited in spatio-temporal coverage. A common method to quantify morphodynamics is shoreline change analysis (SCA, Burningham and Fernandez-Nunez 2020). Currently, SCA often relies on data from beach surveys along pre-defined transects or manual interpretation of orthophotos (Boak and Turner 2005, Dolch 2010). Also, more advanced methods such as photogrammetry or Light Detection and Ranging (LiDAR) surveys with drones or airplanes are increasingly often employed to acquire data with high accuracies (Casella et al. 2020, Christiansen 2021). However, these methods are either labour-intensive and limited in coverage or relatively expensive, often leading to infrequent data collection (Boak and Turner 2005, Apostolopoulos and Nikolakopoulos 2021, Christiansen 2021).

Satellite Earth Observation (EO) data can address these limitations by offering a cost-effective solution for large-scale shoreline monitoring with frequent revisits (Vitousek et al. 2023). For example, data of the Sentinel-2 satellite constellation of the European Space Agency (ESA) is distributed under an open data license, keeping the costs of data analysis inherently low (ESA 2015). Sentinel-2 offers a 10–60 m spatial resolution with a revisit time of 5 days at the equator and 2–3 days in northern Europe, theoretically enabling near-real time detection of shoreline change. The daily growing archive and continuation of the program in coming decades make this program particularly interesting for shoreline monitoring.

However, despite the advantages of EO data, using it for shoreline monitoring presents its own set of challenges. The substantial data volumes of satellite archives, even for relatively small study areas, pose significant technical challenges, requiring substantial computational resources (Vitousek et al. 2023). To effectively manage these large datasets and maintain a reasonable level of effort for processing the data, a high degree of automation is necessary, including data selection and preparation, shoreline extraction and change analysis. Several automated methods for land-water segmentation have been developed, most importantly spectral water indices, which enhance the contrast between land and water (Toure et al. 2019, Apostolopoulos and Nikolakopoulos 2021). Combining these indices with fixed or adaptive thresholding techniques allows to automatically identify the land-water boundary in EO data. In recent years, approaches to delineate the shoreline along the land-water boundary with sub-pixel accuracy have emerged (Hagenaars et al. 2018, Bishop-Taylor et al. 2019).

The increasing availability of cloud-computing platforms, particularly the Google Earth Engine, opened new possibilities, such as first global-scale studies on shoreline change (Luijendeijk et al. 2018, Mentaschi et al. 2018). However, achieving the highest possible accuracy in shoreline extraction requires careful selection of water indices and parameter settings, which vary depending on environmental factors like coastal landforms and water characteristics (Bishop-Taylor et al. 2019, Schütt 2022). Thus, EO-based shoreline monitoring at regional scales should ideally be tailored to the specific conditions of the study area.

To address these challenges, we developed the Shoreline Change and Analysis Tool (SEaCAT), a flexible, sensor-agnostic semi-automatic pipeline that optimises the entire

process from data ingestions to shoreline extraction. SEaCAT extends similar shoreline extraction toolkits, such as CoastSat (Vos et al. 2019) or CoastSeg (Fitzpatrick et al. 2024) by an integrated, highly automated shoreline change analysis module and further offers interactive quality screening, data exploration and visualisation. The pipeline leverages cloud-computing technology to efficiently manage large volumes of satellite data without the need to download raw data. By automating key steps, such as the identification of suitable scenes, shoreline extraction and shoreline change analysis, our approach minimises labour-intensive aspects of EO-based shoreline monitoring while maintaining a high level of accuracy. This integrated, scalable, and transferable approach enables EO-based shoreline monitoring across large spatial and temporal scales.

In this study, we demonstrate our approach by analysing the impacts of the October 2023 storm surge on the German Baltic Sea coast. We focus on two study areas: one in Schleswig-Holstein and the other in Mecklenburg-Vorpommern. In both study areas, we delineate shorelines from the entire Sentinel-2 archive (July 2015 to June 2024) and use this data to analyse the surge's effect on coastal morphology, considering both longer-term variability and trends, identify erosion hotspots and monitor post-storm recovery. Finally, we use our findings to critically assess the potential of EO-based shoreline monitoring to supplement existing monitoring efforts.

2 Methods

2.1 Study areas and the October 2023 storm surge

We chose two study sites at the German Baltic Sea, which were exposed to the easterly winds and waves of the October 2023 storm surge (Figure 1).

The first study area, "Angeln", is located in the federal state of Schleswig-Holstein and extends about 18 km between the two sand spits Geltinger Birk in the north and Schleimünde in the south (Figure 1B). It mainly consists of beaches with narrow dunes or beach ridges and a 3 km long eroding soft cliff (Haffskoppel) in the centre of the study area (Ziegler and Heyen 2005, LKN.SH 2020). The net long-shore sediment transport splits at this cliff and is directed away from it (Eiben 1992). The cliff thus acts as major sediment source, together with inputs from submarine abrasion platforms (Averes et al. 2021). Large parts of this study have no erosion control, except three groin fields (Hasselberg, Oehe, Schleimünde) and few revetments.

The second study area is located on the "Mönchgut" peninsular on the island of Rügen, Mecklenburg-Vorpommern (Figure 1C). It extends 18 km from the town of Sellin in the North to the southern-most point of the peninsular, Südperd, and features a series of wide sandy beaches and four cliffs: Granitz, Nordperd, Lobber Ort, and Südperd (arranged from north to south). Erosion control primarily involves regular beach nourishments between the towns of Göhren and Thiessow (StALU 2021). In some sections of the cliff coast, ripraps, revetments, and detached breakwaters are employed, while in others erosion is permitted to provide sediment for nearby beaches.

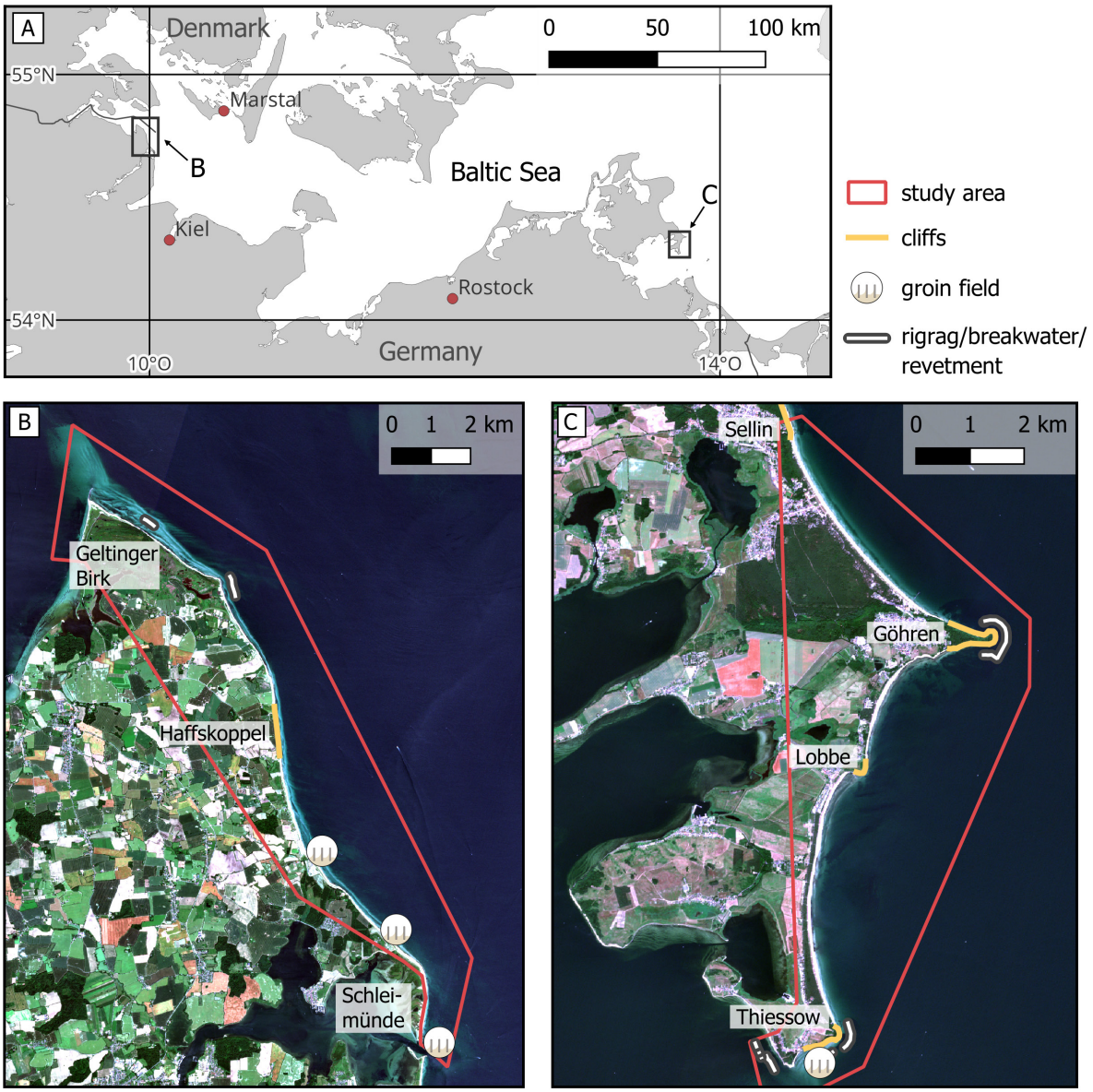

Figure 1: Study areas. A: Overview map of the German Baltic Sea coast. Locations of the subsets B and C are outlined in black. B: Study area "Angeln". C: Study area "Mönchgut". CRS: in A WGS84, in B: UTM32N, in C: UTM33N. Background maps in B and C are Sentinel-2 True Colour RGBs.

In the second half of October 2023, prolonged north-east to easterly gale-force winds over the Baltic Sea caused a severe storm surge along the German Baltic Sea coast (Kiesel et al. 2024). The duration of the event and peak water levels increased from east to west. At Thiessow (study area Mönchgut), the tide gauge recorded a surge duration of 22 hours and a peak water level of 130 cm above mean sea level (MSL), which is categorised as moderate storm surge in the German Baltic Sea (Figure 2A). The tide gauge at Schleimünde (study area Angeln) registered a peak water level of 207 cm above MSL, the highest recorded at this station since 1904 (MELUND 2022). The surge duration at this station was 45 hours, of which 16 hours were a severe storm surge (> 150 cm above MSL).

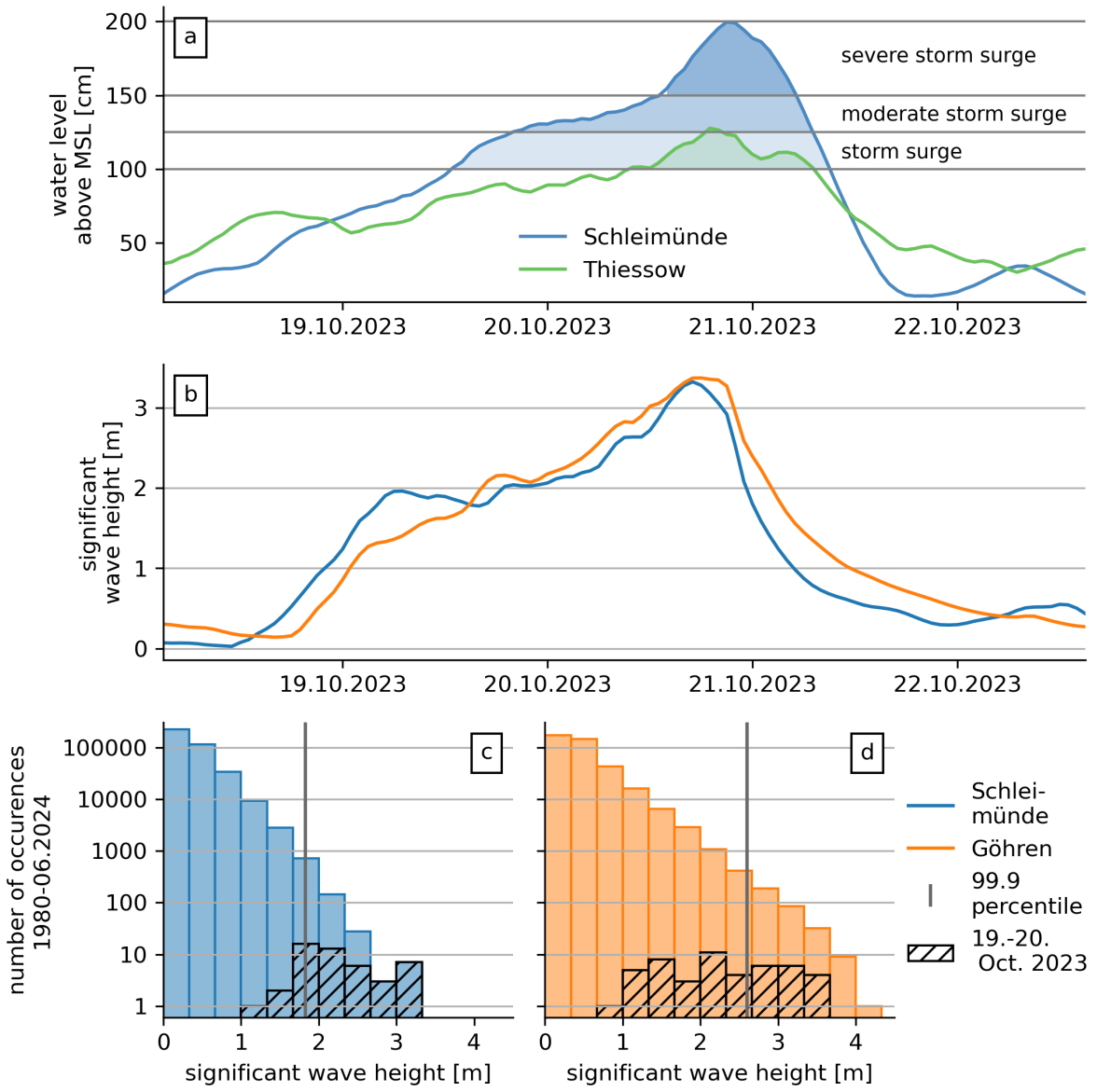

Figure 2: Water level measurements and modelled wave heights during the 2023 storm surge. A: Water levels at the tide gauges of Schleimünde (study area Angeln) and Thiessow (study area Mönchgut). The timeseries are smoothed to hourly means for better readability. Indicated storm surge categories follow the definitions of the Federal Maritime and Hydrographic Agency (BSH). Tide gauge data were provided by the Federal Waterways and Shipping Administration (WSV), made available by the Federal Institute of Hydrology (BfG). B: Significant wave height data for locations off Schleimünde (study area Angeln) and Göhren (Mönchgut). C and D show the distribution of wave heights since 1980 off Schleimünde and Göhren, respectively. Wave height distributions of the 19. and 20.10.2023 are shown in black. Note the logarithmic scale on the y axis. See Lindgren et al. (20024) for more details on the wave model.

The gale-force winds from north-easterly and easterly directions generated large waves in the south-western Baltic Sea. Figure 2B-D present modelled wave height data for both study areas from a hindcast model (Lindgren et al. 2024). While the maximum significant wave height near the shore during the storm surge were similar in both study areas (~ 3.3 m, Figure 2B), this was the highest wave height modelled in the Angeln study area since 1980 (Figure 2C), exceeding previous events by about 70 cm. Generally, the Mönchgut study area experiences a higher-energy wave climate than in Angeln. Although

similar and even stronger wave events have been observed on a decadal timescale, wave heights during the October 2023 storm surge partially exceeded the 99.9 percentile and can thus still be categorized as extreme (Figure 2C and D).

2.2 SEaCAT

We developed SEaCAT for fast semi-automatic monitoring of shoreline changes based on satellite imagery. SEaCAT includes a multi-step workflow for shoreline delineation including selection of suitable satellite images for a given region and time range of interest and subsequent extraction of the land-water boundary based on spectral indices, achieving subpixel accuracy of about one-third of the satellite's spatial resolution in microtidal environments (Schütt 2022). Subpixel co-registration of satellite images can be achieved using AROSICS (Scheffler et al. 2017). Multiple quality screening and filtering steps ensure reliable results. Shoreline change can then be quantified by a set of traditional and newly developed algorithms. SEaCAT is implemented in Python and builds on the xcube data cube toolkit (xcube developers, n.d.) and its Sentinel Hub API integration for accessing satellite image archives in the cloud, while also allowing to easily analyse raster datasets from other sources. Extensive sensitivity analysis and validation of this tool was conducted in Schütt (2022).

Here we used SEaCAT to derive SDS from the entire Sentinel-2 archive (August 2015 to June 2024) for both regions of interest, respectively.

Initially, we selected all Sentinel-2 scenes with less than 20% cloud cover along the coastline and water levels within ± 30 cm of mean sea level (MSL) at acquisition time using local gauge data. The gauge data were provided by the Federal Waterways and Shipping Administration (WSV), made available by the Federal Institute of Hydrology (BfG). The scene selection based on the water level ensures to capture longer-term shoreline change and avoid outliers caused by extreme water level events. The influence of residual water level-related biases on individual SDS and derived trends will be discussed later.

A manual quality screening excluded scenes with residual cloud contamination along the shoreline and those with breaking waves, which introduce bias to SDS positions (Hagenaars et al. 2018).

SEaCAT extracts shorelines from the selected scenes by first emphasizing the contrast between land and water using a spectral water index and then generating the land-water boundary line using the marching squares algorithm (Cipolletti et al. 2012) in combination with Otsu's adaptive thresholding (Otsu 1979). Previous validation efforts of SEaCAT tested six water indices (NDWI (McFeeters 1996), MNDWI (Xu 2006), AWEInsh (Feyisa et al. 2014), MuWI (Wang et al. 2018), ANDWI (Rad et al. 2021) and the NIR-Blue Normalized Index, NBNI) at six validation sites in the Baltic Sea and the North Sea against reference shorelines from laser scans and orthophotos (Schütt 2022). In the Baltic Sea, NBNI performed best and was selected as spectral water index in this study. It utilizes the strong contrast of water reflectance in different parts of the electromagnetic spectrum and is defined as:

$$NBNI = \frac{Blue - NIR}{Blue + NIR} \quad (1)$$

The marching squares algorithm is used to generate contour lines from a two-dimensional grid of scalar values along a provided threshold. It iterates over the grid and linearily interpolates the position of the contour line within each cell based on the values at the cell corners. For example, if two adjacent cell corners, c1 and c2, have values of 0.0 and 1.0, and the threshold is set to 0.8, the contour line would be placed at 80% of the distance between c1 and c2. This interpolation enables the extraction of contour lines with sub-pixel precision and results in a smooth representation of the shoreline (Bishop-Taylor et al. 2019, Vos et al. 2019). For each image we determined the optimal NBNI threshold for shoreline detection using Otsu's adaptive thresholding. At validation sites most similar to our study areas, a sandy beach and a cliff coast close to the city of Kiel, the mean absolute error of this setup was 2.9 and 3.5 m and the bias 0.7 and 2.5 m, respectively, compared to shorelines derived from LiDAR data and orthophotos (Schütt 2022).

We quantify shoreline change with our proposed Directional Buffer Overlay method (DBO). This approach combines the strengths of traditional methods like the transect-from-baseline (TFB) and the buffer overlay (BO; Heo et al. 2009) methods while mitigating their respective weaknesses, including TFBs sensitivity to baseline and transect definition (Khallaghi and Pontius 2022) or BOs inability to specify the change direction (Heo et al. 2009). DBO first divides the coast into small segments. In this study, we used a spacing of 100 m between the transects. In each segment, a series of buffers is used to determine the average shoreline shift between consecutive shoreline observations, creating a time series of a shorelines' cross-shore position. These time series are then analysed statistically to quantify shoreline change. The segmentation of the coastline is broadly based on Jackson et al. (2012) but optimised for automation (Figure 3). Alternatively, user-defined baselines and transects can be used for the analysis.

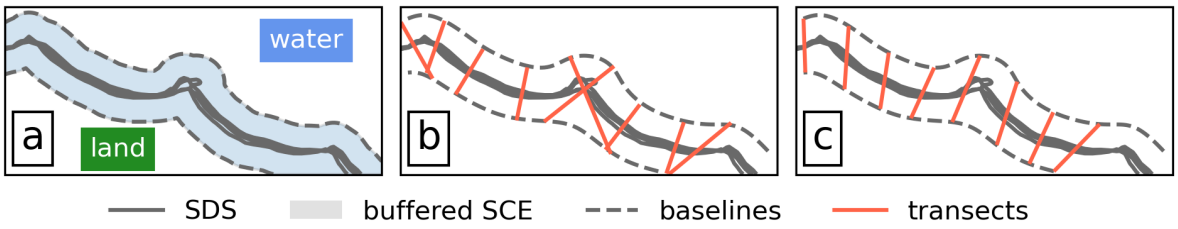

Figure 3: Automatic baseline and transect generation in SEaCAT. A: Seaward and landward baselines are generated around the buffered shoreline change envelope (SCE). B: Baselines are smoothed with a Gaussian filter and transects are generated perpendicular from the seaward to the landward baseline. C: Smoothing of the transects azimuth and filtering removes crossing transects.

After segmenting the coastline, a modification of the BO method (Heo et al. 2009) is used within each segment to estimate the average shoreline displacement between consecutive SDS. A single-sided buffer is created on the seaward side of the first observation with a width much smaller than the satellites pixel resolution (Figure 4). In this study, we used an increment of 1 m. We then determine the length of the new shoreline inside the buffer and store this value. This procedure repeats iteratively as the buffer moves away from the first shoreline observation until no parts of the new shoreline are within the buffer. The procedure is mirrored on the inshore side of the first shoreline observation with erosional shifts stored as negative values. This iterative buffering derives the probability density function (PDF) of distances between the two lines, accounting for the shift direction.

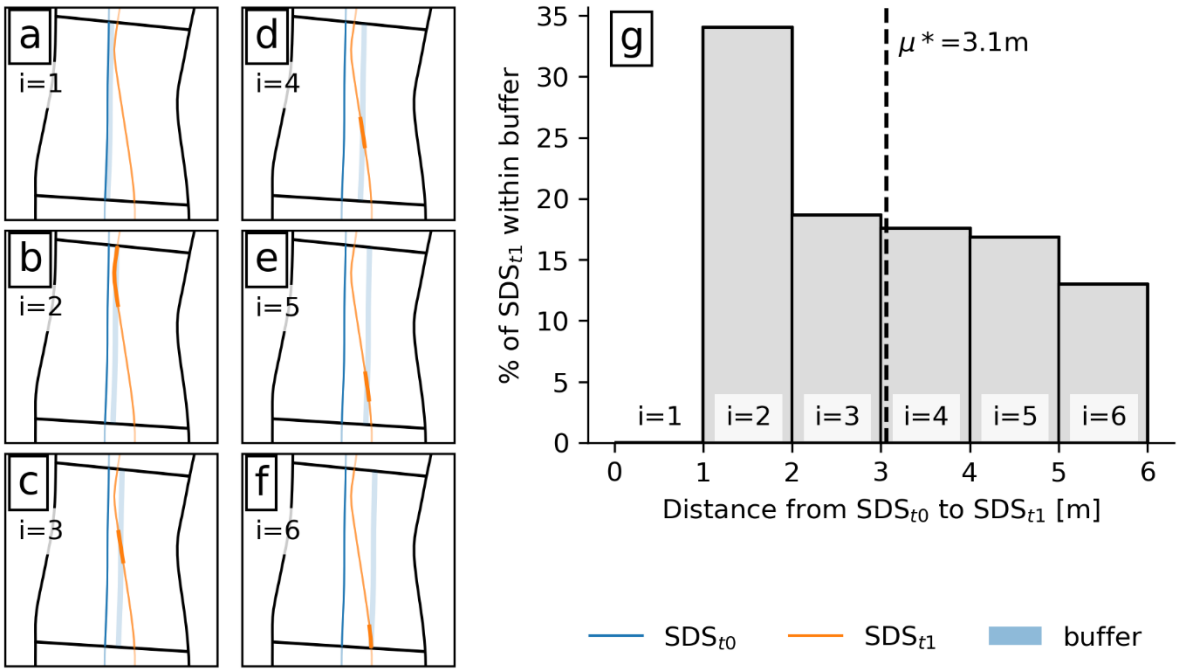

Figure 4: Schematic diagram of the distance measurements with DBO. In this example, we measure the distance from SDS_{t0} and SDS_{t1}. A-F show the moving buffer from SDS_{t0} in each iteration i. The part of SDS_{t1} in the buffer is indicated in bright. G shows the histogram of the distances between SDS_{t0} and SDS_{t1}. The dashed line indicates the weighted average distance (μ*).

We derive the average shoreline shift between the two lines by calculating the weighted average of this distribution:

$$\mu^* = \frac{\sum_{i=1}^{N} x_i \omega_i}{\sum_{i=1}^{N} \omega_i} \quad (2)$$

where μ^* is the weighted mean distance, N the number of bins in the distance distribution, x the centre distance of a bin and ω the proportion of the new shoreline observation within a bin.

Sensitivity analysis of DBO have proven the robustness of this method (Schütt 2022). In contrast to the TFB method, DBO is not sensitive to the definition of baselines, which is a prerequisite for automatic SCA. Moreover, the increment in the buffer analysis has insignificant influence on derived distances if it is < 20% of the pixel resolution.

To estimate shoreline changes over time, SEaCAT runs DBO iteratively for each consecutive pair of observations in the time series to generate a time series of cross-shore positions. To quantify shoreline change, we derive five key measures, including Net Shoreline Movement (NSM), Shoreline Change Envelope (SCE), end-point rate (EPR) and linear regression rate (LRR; see Burningham and Fernandez-Nunez (2020) for definition and discussion).

In this study, we focus on the LRR, which reflects the time averaged linear trend of shoreline change. To ensure the reliability of LRR calculations for any subset of the dataset, we verify that the distribution of water levels in the subset is consistent with that of the entire timeseries by performing a Kolmogorov–Smirnov test ($p > 0.05$).

3 Results

3.1 Angeln

After filtering for water level, cloud cover, and completing the final manual quality control, we retained 125 SDS observations in the Angeln study area from the Sentinel-2 archive, from which the change of the coastline was determined. In three small areas, shadows from tall trees near the shoreline were misclassified as land by our water index. These areas were masked to exclude erroneous SDS from further analysis.

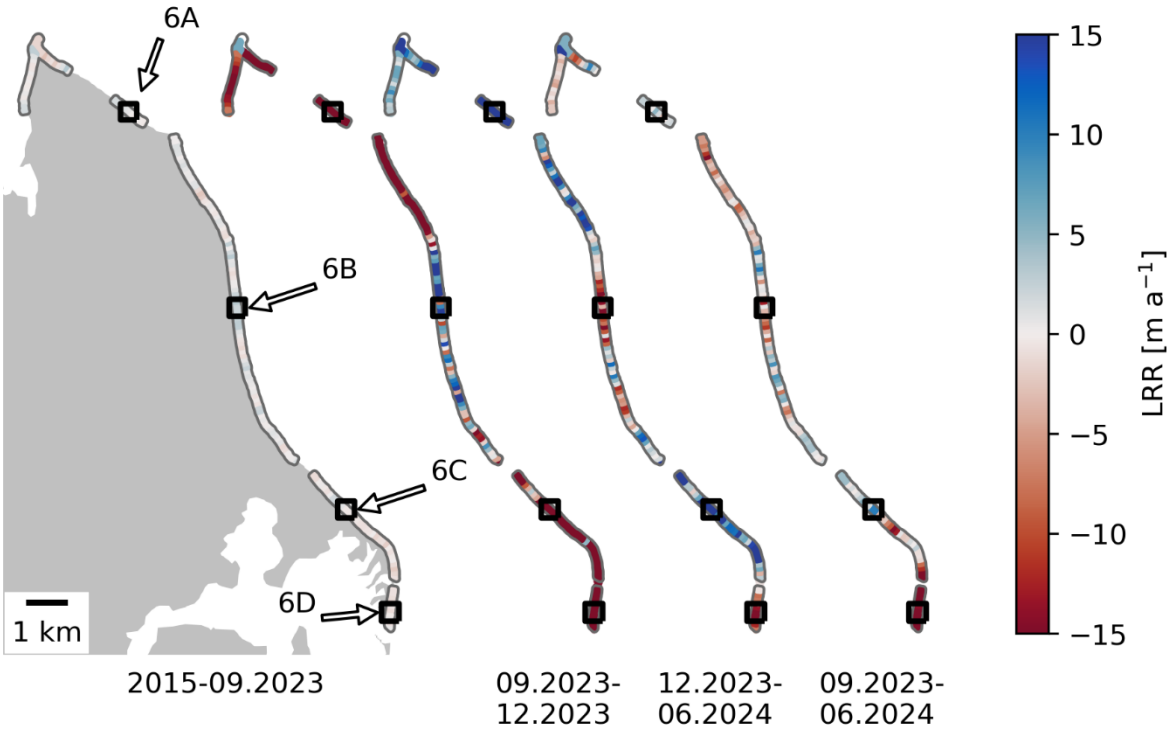

Figure 5: Linear shoreline change rates (linear regression rate, LRR) in the Angeln study area derived with SEaCAT for different periods (left to right): baseline period, immediate post-storm surge, stabilization phase and post-storm recovery phase. Negative (positive) trends, i.e. erosion (accretion) are shown in red (blue). Black boxes show the locations of the cross-shore shoreline subsets in Figure 6.

Our SCA reveals distinct patterns of gradual erosion and accretion in the baseline period prior to the October 2023 surge event (Figure 5). Average absolute change during the eight years before the surge were lower than one m a^{-1}. Since the surge, morphological change has accelerated. In the post-storm recovery phase between September 2023 and June 2024, 64% of the studied coastline showed a shoreline retreat. Erosion hotspots are the Schleimünde sand spit and the coastline between Haffskoppel and Geltinger Birk. The centre of the study area, i.e. the Haffskoppel cliff and adjacent beaches, shows complex patterns of erosion and accretion.

In the immediate post-storm period, i.e. the initial three months after the surge until December 2023, significant erosion especially in the northern and southern part of the study area can be observed, while at the Haffskoppel cliff we registered shoreline advance (Figure 5 and Figure 6B). In the following stabilization phase between December 2023 and

June 2024, trends reversed in most places, indicating a beginning shoreline recovery. At Schleimünde, however, erosion continued at fast rates until May 2024 (Figure 6D).

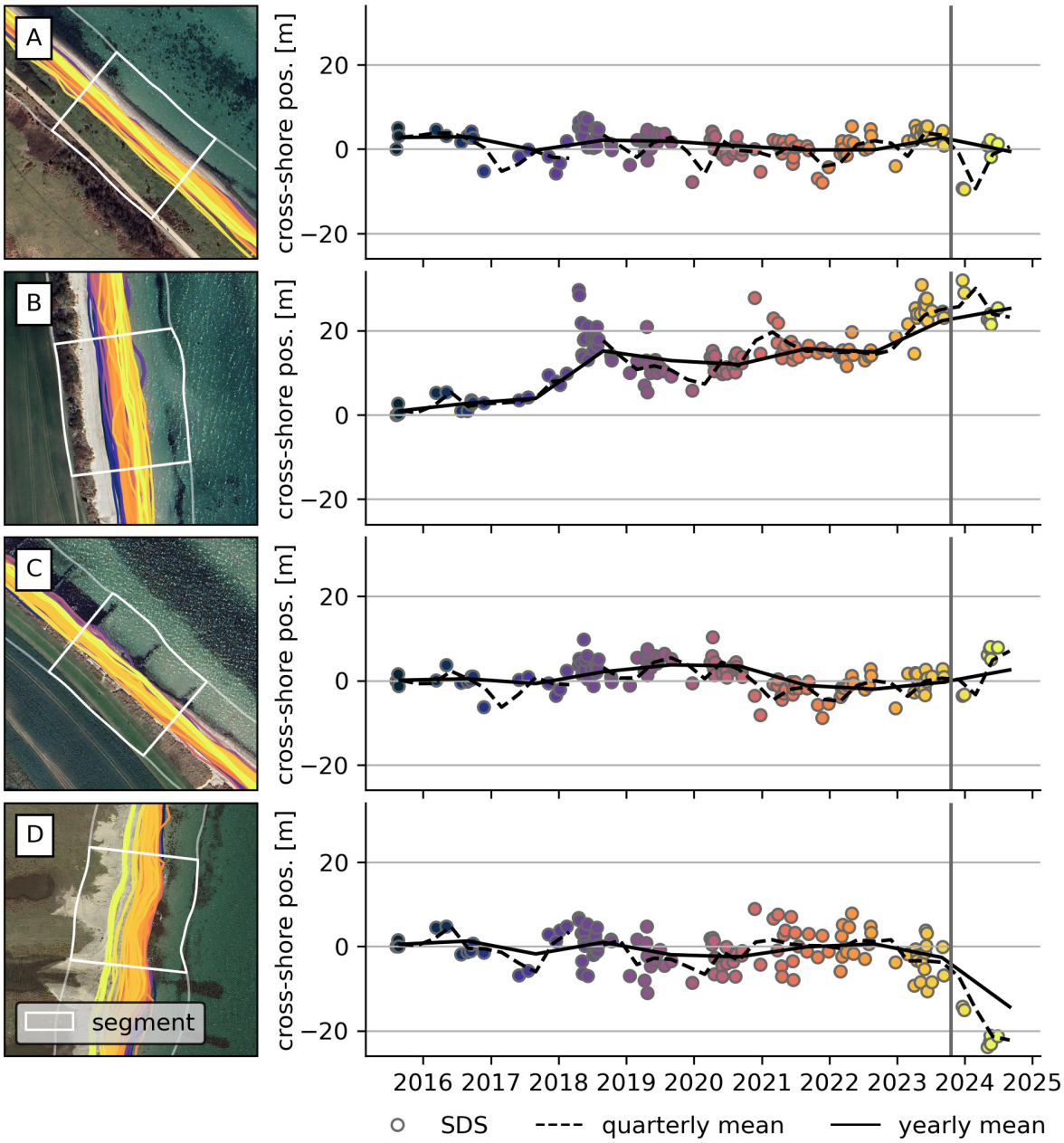

Figure 6: Cross-shore shoreline positions in selected segments of the Angeln study area. Locations of each segment are indicated in Figure 5. The left column shows delineated shorelines, the right column provides cross-shore positions of each shoreline observation. Colour coding indicates the time of a shoreline observation. The vertical grey line in the right column indicates the October 2023 storm surge.

3.2 Mönchgut

After our quality control, 118 SDS since July 2015 remained in our dataset, including 9 observations collected after the October 2023 storm surge. We masked two sections of the coast were shadow confusion along north-facing cliffs impaired our SDS results.

The baseline period in Figure 7 highlights long-term erosion patterns at the Lobbe cliff and the southernmost point at Thiessow before the October 2023 surge (see also Figure 8D). Our SCA also reveals positive shoreline change rates along the beaches between Göhren and Thiessow. However, a closer inspection reveals that these positive change rates can be attributed to single shoreline advancements in 2017 (Figure 8C) and 2021 (Figure 8B).

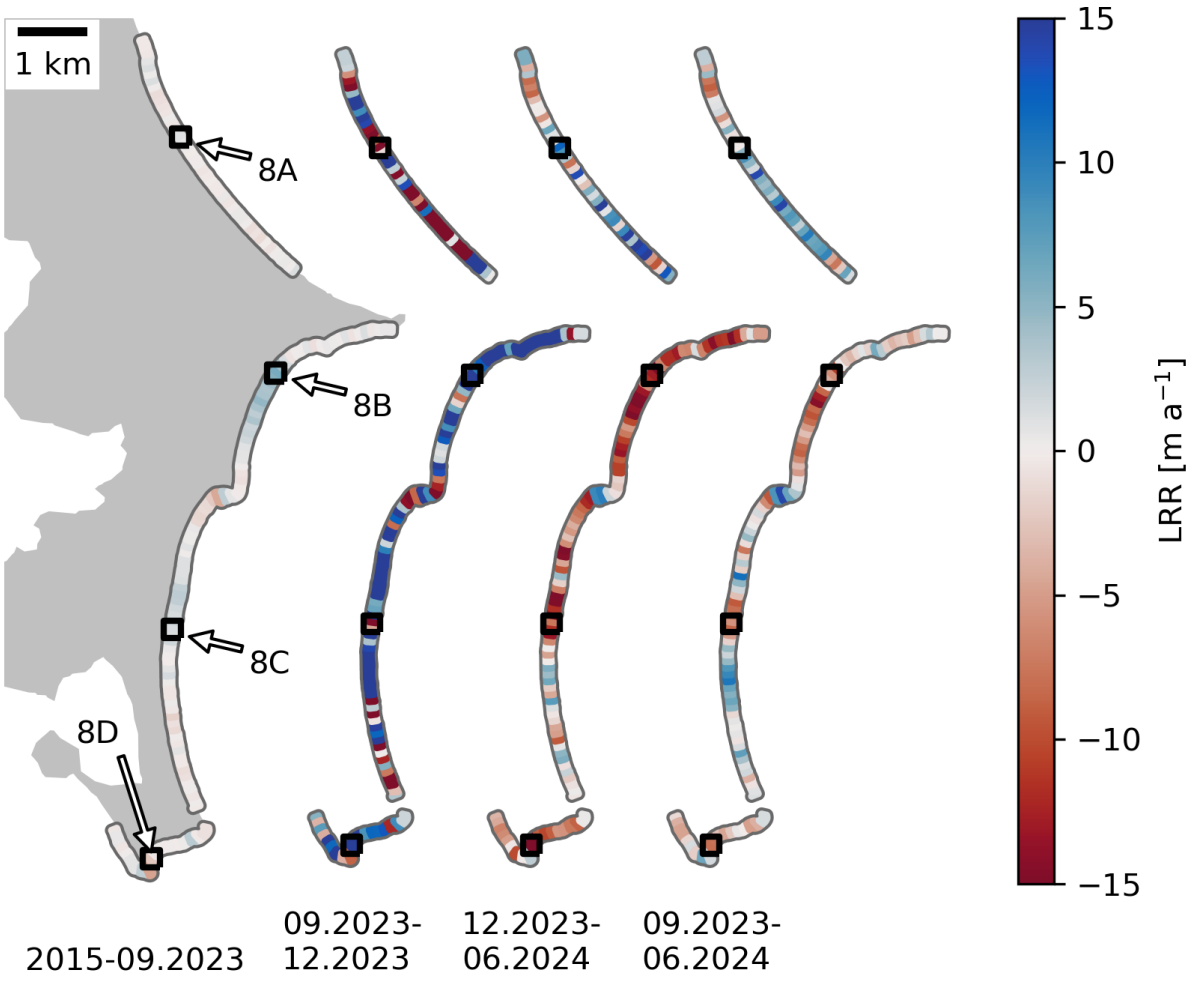

Figure 7: Linear shoreline change rates at Mönchgut derived with SEaCAT for different periods (left to right): baseline period, immediate post-storm surge, stabilization phase and post-storm recovery phase. Black boxes in A show the locations of the cross-shore shoreline subsets in Figure 8.

After the surge, our SCA reveals net shoreline retreat along half of Mönchguts coastline in the post-storm recovery phase until June 2024 (Figure 7). Erosion is especially evident at the beach between Göhren and Lobbe (Figure 8B), while we observe net accumulation at beaches north of Göhren and north of Thiessow. However, initial changes after the surge until December 2023 show an almost reversed pattern with erosion north and accumulation south of Göhren. This suggests that the October 2023 storm surge had only a short-term impact on coastal morphology, with most changes being reversed over the following months. This is further supported by the cross-shore positions in Figure 8, which suggest that effects of this event were within the range of longer-term variability.

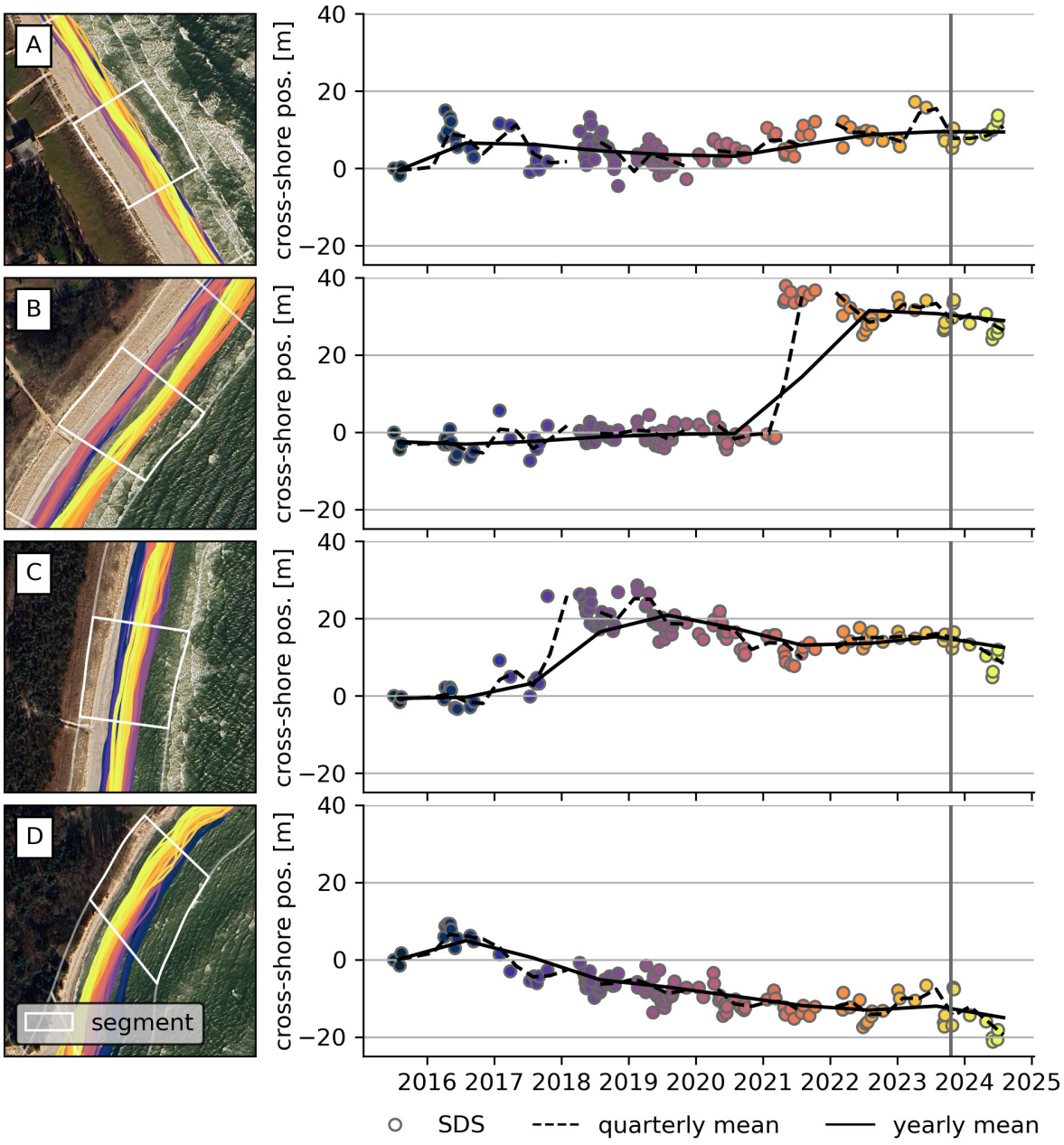

Figure 8: Cross-shore shoreline positions in selected segments of the Mönchgut study area. Locations of each segment are indicated in Figure 7. The vertical grey line indicates the October 2023 storm surge. The figure follows the same format as Figure 6.

4 Discussion

4.1 Effects of the storm surge on coastal morphodynamics

The degree of impact of the October 2023 storm surge differs considerably between our two study sites. It is significantly larger in the more westerly Angeln study area than at Mönchgut, where morphological changes caused by this event are within the range of morphodynamics observed since 2015. This pattern cannot be attributed solely to wave heights, as these were comparable in both study regions (Figure 2B). However, given Mönchgut's

higher-energy wave climate, it is plausible that its beaches feature an adapted sediment distribution and slope, which may have contributed to a greater resilience to the storm surge (Angnuureng et al. 2017). Furthermore, both longer surge duration and peak water levels created a higher morphodynamic potential in Angeln (Figure 2, Łabuz and Kowalewska-Kalkowska 2011). In Angeln, water levels exceeded those of a 200-year event by approximately 10 cm, while in Mönchgut, they were about 30 cm lower than a 200-year event (Kiesel et al. 2024).

In the Angeln study area, the Schleimünde sand spit showed the most significant morphological changes, characterized by an accelerated shoreline retreat lasting until approximately six months after the event. This can likely be attributed to drastic changes in the horizontal profile of the spit, which were reported by early on-site investigations (pers. comm. Christian Winter, 23.08.2024). Wind and waves destabilized beach ridges in the east of the spit, moving a considerable volume of material from the beach ridges westward, burying vegetation underneath (Figure 9). Therefore, the profile at the shoreline to the open Baltic Sea flattened, causing a westward movement of the shoreline. Three minor storm surges in January and February 2024 (highest water level 116 cm above MSL) likely contributed to further shoreline retreat. True colour satellite images suggest that the spit profile is not reverting to its pre-surge shape, indicating a lasting change of the spit's morphology (Figure 9C). A more in-depth analysis of this area with altimetry data is needed to verify this hypothesis, quantify volumetric change and investigate potential implications for the spits mid- and long-term structural resistance.

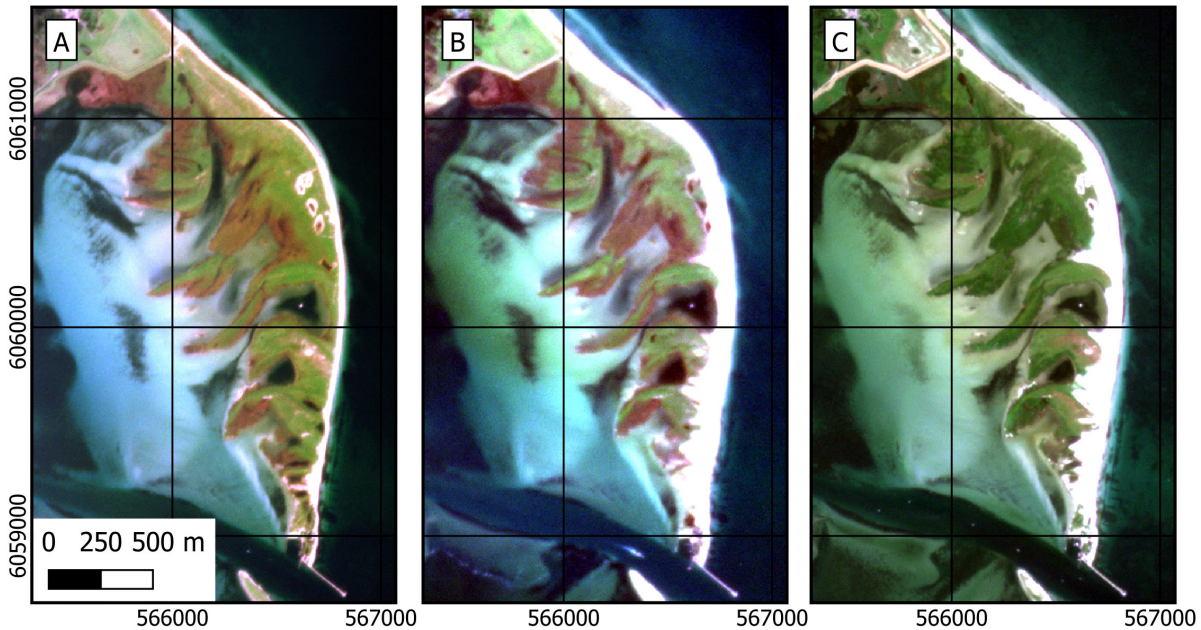

Figure 9: True Colour RGB Planet SuperDove images of the Schleimünde sand spit (Planet Labs 2024). A: Before the surge (18.10.2023). B: Immediately after the surge (23.10.2023). C: 8 months after the storm surge (25.06.2024). CRS: UTM32N/WGS84 (EPSG:32632).

The centre of the Angeln study area shows a complex pattern of erosion and accretion directly after the storm surge. This is likely an effect of local cliff collapses at Haffskoppel, which released new material into the system and may initially move the shoreline seaward (Brooks and Spencer 2010). This effect can also be observed in previous years: notable shoreline advancements in April 2018, November 2020, and May/June 2023 follow storm

surges or wind storms from easterly directions shortly before the shoreline observation (BSH 2018, 2020, 2023).

The eroded cliff material initially deposited in front of the cliff toe is redistributed according to its grain size and transport capacity in both cross-shore and long-shore sediment transport directions (Averes et al. 2021). The long-shore sediment transport splits at Haffskoppel, allowing the redistribution of material to both northerly and southerly directions (Eiben 1992). The material deposits in sink areas such as the sand spit at Geltinger Birk or the groin field in Figure 6C. This highlights the importance of cliffs as sediment source for this sediment-starved environment (Averes et al. 2021).

The widespread shoreline recovery along the sandy beaches in the months following the surge (Figure 5) is further supported by a reduction of average wave energy during spring and summer. This seasonal effect causes a beach profile transition from a narrower beach during winter to a wider beach during summer, as net onshore transport of material stored in nearshore bar systems increases (Schwarzer et al. 2003, Senechal and Ruiz de Alegría-Arzaburu 2020). Evidence for this seasonal effect along sandy beaches in the Angeln study area can be seen in the years before the 2023 surge in subsets A, C and D of Figure 6.

In the Mönchgut study area, linear change rates observed in the shorter periods following the storm surge deviate considerably from the long-term changes since 2015 (Figure 7). However, cross-shore positions in Figure 8 do not indicate a substantial or only a short-lived impact of the storm surge on the shoreline. Considering the comparably low intensity of the storm surge and the likely higher resilience of beaches in the Mönchgut study region to wave events of this magnitude, it is not surprising that the shoreline changes induced by the October 2023 storm surge fall within the range of observed long-term morphodynamics. The higher change rates seen after the surge in Figure 7 can be attributed to the brief assessments periods, which capture short-term, event-driven alterations leading to exaggerated rates of shift when extrapolated to annual rates. Among these events is, despite the October 2023 surge, one other storm surge in January 2024 (103 cm above MSL) and 14 events with elevated water levels (50 cm < water level < 100 cm). Other likely contributing elements include seasonal changes in wave patterns (Siewert et al. 2015) or precipitation-driven cliff collapses, which often have a phase lag after triggering events (Dietze et al. 2020).

Although the morphodynamic effects of the October 2023 surge were low in the Mönchgut study area, our data reveals other distinct morphodynamic patterns. Specifically, along many parts of the exposed beaches between Göhren and Thiessow, we observed short-term accretionary events of large magnitude, which temporarily offset otherwise negative shoreline trends. These can be attributed to single beach nourishments in 2017 (Figure 8C) and 2021 (Figure 8B). Nourishments of these beaches are carried out regularly to compensate sediment deficits in this area (StALU 2021). The nourishments shifted the shoreline seaward by approximately 20-35 meters. These single events mask the longer-term trend of erosion, which can be observed after the nourishments at both beaches. That coastal morphodynamics in this area are dominated by nourishments is typical for soft coasts of Mecklenburg-Vorpommern, where annual nourishment volumes amount to about 0.5 million m^3/a (StALU 2021, Tiede et al. 2023). The trends of erosion after the nourishments further underscore the need for regular nourishments for preserving the beach. At the same time, regular nourishments can create a misleading sense of security regarding coastal hazards, possibly inflating property values (Gopalakishnan et al. 2011)

and encouraging both investments and relocations into the coastal zone, which in turn increases coastal risks (Tiede et al. 2023).

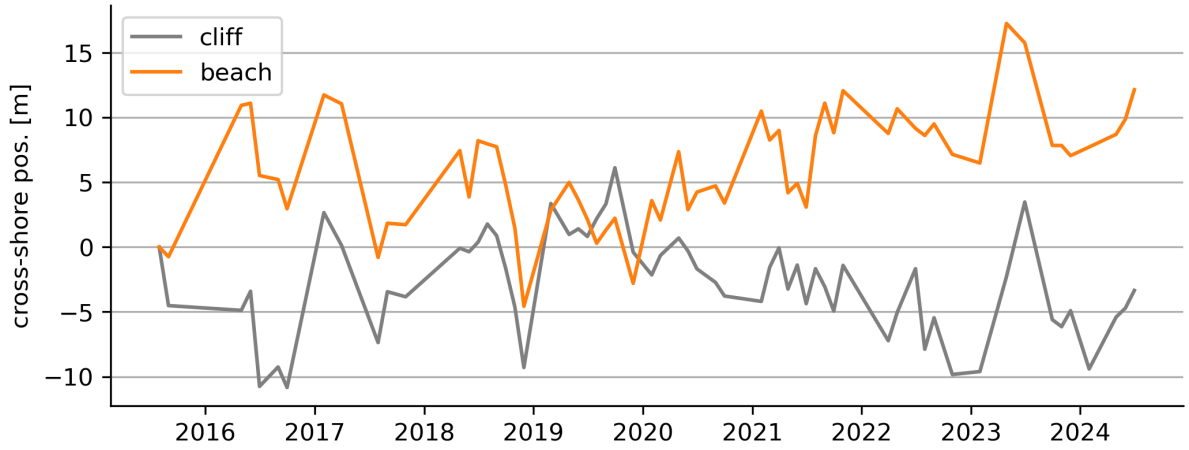

Figure 10: Mean monthly shoreline position of a cliff segment (north-west corner of the study area) and the beach segment from Figure 8A.

The beach between Göhren and Sellin is not nourished, however, it shows no major trends since 2015 (Figure 7, Figure 8A). Material eroded at the unprotected Granitz cliff at Sellin supplies this beach and compensates losses (pers. comm. Ulrich Floth, 23.07.2024). In fact, the significant negative correlation between shoreline positions of the Granitz cliff and the beach, support this interpretation (Figure 10, Pearson $R = -0.51$, $p << 0.005$ at two months lag).

The peninsular at Thiessow is well protected against coastal erosion by rigrags, breakwaters and groins. Low long-term erosion rates (2015 to 2023) suggest that this concept works well. Only exception is the unprotected beach in Figure 8D, which erodes since at least 2016. It appears that a reduced sediment supply from the nearby protected cliffs cause this shoreline retreat.

4.2 Considerations of EO-based shoreline monitoring at regional scales

We presented the potential of earth observation for describing, analysing and interpreting morphological changes in the coastal zone by using the semi-automated toolkit SEaCAT. SEaCAT enables to monitor largescale trends as well as identify hotspots of short-term shoreline change. The analyses are based on the water-land boundary lines depicted from individual satellite images and in combination with information on water level at the time of acquisition, morphological processes can be described. Thus, the detection of seasonal and long-term dynamics can supplement existing monitoring data, although the often high cloud coverage in northern Germany limits available observations. Nevertheless, we derived, on average, more than 13 shoreline observations per year in both study areas, which allows to evaluate the impact of, for instance, a storm season or even a single event.

We achieve these frequent observations by tolerating water levels of MSL ±30 cm at satellite acquisition. This range introduces potential water level-related biases in individual shoreline positions. Therefore individual measurements should be treated with caution. However, aggregating multiple observations in trend analysis helps to average out these biases, enabling increasingly robust change analysis as the number of observations grows

(Xu 2018). While this approach is particularly suited to micro-tidal environments, strict water level filtering in a macro-tidal environment would drastically reduce the number of available observations (Schütt 2022), or require a tidal correction of the shoreline position using beach slope data (Vos et al. 2020).

Although a manual quality screening of all shorelines is still required, the availability of Sentinel-2 data for low or no costs (depending on the data source), high automation level and robustness of SEaCATs shoreline extraction and change analysis make it a fast and cost-effective tool for shoreline monitoring. Even more accurate SDS could potentially be derived from commercial very-high resolution data, although regular acquisitions with VHR satellites would significantly increase costs of our approach (Burningham and Fernandez-Nunez 2020, Smith et al. 2021).

SDS accuracy from Sentinel-2 is not as high as methods currently employed for shoreline monitoring (LiDAR/ALB scans or manual delineation in high-resolution aerial imagery; Christiansen 2016, Smith et al. 2021). It also lacks information in the vertical dimension, which LiDAR offers. EO-based shoreline monitoring can thus not replace those traditional methods but can help to use them more efficiently by identifying priority areas for monitoring and defining optimal revisit times for flight campaigns. Especially its comparably frequent observations at low costs makes it a reasonable addition to existing monitoring methods.

We have shown that access to the Sentinel-2 archive (since 2015) allows to retrospectively derive baselines and assess longer-term dynamics and trends of coastal development. The high availability of data combined with an accuracy suitable for trend and change analysis provides additional information that closes temporal data gaps of local or large-scale aerial surveys. Particularly in areas with relatively minor morphological changes, such as the Baltic Sea coast, the coastal protection administrations, the waterway and shipping administrations and the Federal Maritime and Hydrographic Agency have correspondingly little coastal data at their disposal. The availability of EO-based information is even more important in remote regions where no monitoring of coastal changes took place in the past.

The observation period of Sentinel-2 can be enlarged with other satellite missions such as the Landsat archive, which goes back to 1982 (Wulder et al. 2019). However, the spatial resolution of 30 m, lower temporal coverage, and higher noise especially in the data from early Landsat sensors provide a lower accuracy of the derived SDS (Apostolopoulos and Nikolakopoulos 2020, Sunny et al. 2022). Nevertheless, larger changes in coastline positions can be derived.

Essentially, SEaCAT provides robust methods to monitor land-water boundaries and quantify their change over time. This offers opportunities for related applications. Notably, SEaCAT is currently also being used to monitor morphodynamics of tidal creek systems in the German Wadden Sea. This demonstrates the method's capability to derive information in remote or inaccessible regions where data is scarce. With small adaptations, the toolkit could also be applied to monitor other linear features, such as dune base lines or even glaciers. Looking ahead, advancements in sensor technology and data analysis will enhance our capabilities for EO-based coastal monitoring. For example, integrating space-born optical and LiDAR sensors like IceSAT-2 now allows to derive near-shore bathymetry and monitor its dynamics without in-situ calibration data (Thomas et al. 2021).

5 Acknowledgements

We gratefully acknowledge Benjamin Franz from the Ministry for Energy Transition, Climate Protection, Environment and Nature (MEKUN), Schleswig-Holstein, and Ulrich Floth from the State Offices for Agriculture and Environment (StALU), Mecklenburg-Vorpommern, for their inspiring discussions and valuable support. We would like to thank the anonymous reviewer for their constructive comments and valuable feedback, which greatly improved this study.

The development of SEaCAT has been largely supported by the ESA funded project Space for Shore.

6 References

Angnuureng, D. B.; Almar, R.; Senechal, N.; Castelle, B.; Addo, K. A.; Marieu, V.; Ranasinghe, R.: Shoreline resilience to individual storms and storm clusters on a meso-macrotidal barred beach. In: Geomorphology, 290, 265–276, 2017.

Apostolopoulos, D.; Nikolakopoulos, K.: Assessment and Quantification of the Accuracy of Low- and High-Resolution Remote Sensing Data for Shoreline Monitoring. In: ISPRS International Journal of Geo-Information, 9, 6, 391, 2020.

Apostolopoulos, D.; Nikolakopoulos, K.: A review and meta-analysis of remote sensing data, GIS methods, materials and indices used for monitoring the coastline evolution over the last twenty years. In: European Journal of Remote Sensing, 54, 1, 240–265, 2021.

Averes, T.; Hofstede, J. L. A.; Hinrichsen, A.; Reimers, H.-C.; Winter, C.: Cliff Retreat Contribution to the Littoral Sediment Budget along the Baltic Sea Coastline of Schleswig-Holstein, Germany. In: Journal of Marine Science and Engineering, 9, 8, 870, 2021.

Bishop-Taylor, R.; Sagar, S.; Lymburner, L.; Alam, I.; Sixsmith, J.: Sub-Pixel Waterline Extraction: Characterising Accuracy and Sensitivity to Indices and Spectra. In: Remote Sensing, 11, 24, 2984, 2019.

Boak, E. H.; Turner, I. L.: Shoreline Definition and Detection: A Review. In: Journal of Coastal Research, 214, 688–703, 2005.

Brooks, S. M.; Spencer, T.: Temporal and spatial variations in recession rates and sediment release from soft rock cliffs, Suffolk coast, UK. In: Geomorphology, 124, 1-2, 26–41, 2010.

BSH: Abflussjahr 2018, Nr.05. Hydrologischer Monatsbericht März 2018 für die Schleswig-Holsteinische und Mecklenburg Vorpommersche Ostseeküste, Rostock: Bundesamt für Seeschifffahrt und Hydrographie, 2018. https://www2.bsh.de/aktdat/wvd/Berichte/Ostsee/A%202018/Monatsbericht%2005%20M%C3%A4rz%202018.pdf, accessed 03.12.2024.

BSH: Abflussjahr 2020, Nr.12. Hydrologischer Monatsbericht Oktober 2020 für die Schleswig-Holsteinische und Mecklenburg-Vorpommersche Ostseeküste, Rostock: Bundesamt für Seeschifffahrt und Hydrographie, 2020. https://www2.bsh.de/aktdat/wvd/Berichte/Ostsee/A_2020/Monatsbericht_12_Oktober_2020.pdf, accessed 03.12.2024.

BSH: Abflussjahr 2023, Nr.07. Hydrologischer Monatsbericht Mai 2023 für die Schleswig-Holsteinische und Mecklenburg-Vorpommersche Ostseeküste, Bundesamt für Seeschiffahrt und Hydrographie, 2023. https://www2.bsh.de/aktdat/wvd/Berichte/Ostsee/A_2023/Monatsbericht_07_Mai_2023.pdf, accessed 03.12.2024.

Burningham, H.; Fernandez-Nunez, M.: Shoreline change analysis. In: Jackson, D. W.; Short, A. D. (eds.): Sandy Beach Morphodynamics, Elsevier, 439–460, https://doi.org/10.1016/10.1016/B978-0-08-102927-5.00019-9, 2020.

Casella, E.; Drechsel, J.; Winter, C.; Benninghoff, M.; Rovere, A.: Accuracy of sand beach topography surveying by drones and photogrammetry. In: Geo-Marine Letters, 40, 2, 255–268, 2020.

Castelle, B.; Masselink, G.: Morphodynamics of wave-dominated beaches. In: Cambridge Prisms: Coastal Futures, 1, 2023.

Christiansen, L.: New techniques in capturing and modelling of morphological data. In: Hydrographische Nachrichten, 105, 11, 22–25, 2016.

Christiansen, L.: Laser Bathymetry for Coastal Protection in Schleswig-Holstein. In: PFG – Journal of Photogrammetry, Remote Sensing and Geoinformation Science, 89, 2, 183–189, 2021.

Cipolletti, M. P.; Delrieux, C. A.; Perillo, G. M.; Cintia Piccolo, M.: Superresolution border segmentation and measurement in remote sensing images. In: Computers & Geosciences, 40, 87–96, 2012.

Dietze, M.; Cook, K. L.; Illien, L.; Rach, O.; Puffpaff, S.; Stodian, I.; Hovius, N.: Impact of Nested Moisture Cycles on Coastal Chalk Cliff Failure Revealed by Multiseasonal Seismic and Topographic Surveys. In: Journal of Geophysical Research: Earth Surface, 125, 8, 2020.

Dolch, T.: Analysis of Long-Term Changes of a Sandy Shoreline Utilising High-Resolution Aerial Photography. In: Green, D. R. (ed.): Coastal and Marine Geospatial Technologies, Springer Netherlands, Dordrecht, 187–196, https://doi.org/10.1016/10.1007/978-1-4020-9720-1_17, 2010.

Eiben, H.: Schutz der Ostseeküste von Schleswig-Holstein. In: Kramer, J.; Rohde, H. (eds.): Historischer Küstenschutz. Deichbau, Inselschutz und Binnenentwässerung an Nord- und Ostsee, Verlag Konrad Wittwer, Stuttgart, 517–534, 1992.

ESA: Sentinel-2 User Handbook, European Space Agency, 2015. https://sentinel.esa.int/documents/247904/685211/Sentinel-2_User_Handbook, accessed 02.09.2024.

Feyisa, G. L.; Meilby, H.; Fensholt, R.; Proud, S. R.: Automated Water Extraction Index: A new technique for surface water mapping using Landsat imagery. In: Remote Sensing of Environment, 140, 23–35, 2014.

Fitzpatrick, S.; Buscombe, D.; Warrick, J. A.; Lundine, M. A.; Vos, K.: CoastSeg: an accessible and extendable hub for satellite-derived-shoreline (SDS) detection and mapping. In: Journal of Open Source Software, 9, 99, 6683, 2024.

Gopalakrishnan, S.; Smith, M. D.; Slott, J. M.; Murray, A. B.: The value of disappearing beaches: A hedonic pricing model with endogenous beach width. In: Journal of Environmental Economics and Management, 61, 3, 297–310, 2011.

Hagenaars, G.; Vries, S. de; Luijendijk, A. P.; Boer, W. P. de; Reniers, A. J.: On the accuracy of automated shoreline detection derived from satellite imagery: A case study of the sand motor mega-scale nourishment. In: Coastal Engineering, 133, 113–125, 2018.

Hallegatte, S.; Green, C.; Nicholls, R. J.; Corfee-Morlot, J.: Future flood losses in major coastal cities. In: Nature Climate Change, 3, 9, 802–806, 2013.

Harley, M. D.; Turner, I. L.; Kinsela, M. A.; Middleton, J. H.; Mumford, P. J.; Splinter, K. D.; Phillips, M. S.; Simmons, J. A.; Hanslow, D. J.; Short, A. D.: Extreme coastal erosion enhanced by anomalous extratropical storm wave direction. In: Scientific Reports, 7, 1, 6033, 2017.

Heo, J.; Kim, J. H.; Kim, J. W.: A new methodology for measuring coastline recession using buffering and non-linear least squares estimation. In: International Journal of Geographical Information Science, 23, 9, 1165–1177, 2009.

Jackson, C. W.; Alexander, C. R.; Bush, D. M.: Application of the AMBUR R package for spatio-temporal analysis of shoreline change: Jekyll Island, Georgia, USA. In: Computers & Geosciences, 41, 199–207, 2012.

Jacobson, C.; Carter, R. W.; Thomsen, D. C.; Smith, T. F.: Monitoring and evaluation for adaptive coastal management. In: Ocean & Coastal Management, 89, 51–57, 2014.

Khallaghi, S.; Pontius, R. G.: Area method compared with Transect method to measure shoreline movement. In: Geocarto International, 37, 20, 5963–5984, 2022.

Kiesel, J.; Wolff, C.; Lorenz, M.: Brief communication: From modelling to reality – flood modelling gaps highlighted by a recent severe storm surge event along the German Baltic Sea coast. In: Natural Hazards and Earth System Sciences, 24, 11, 3841–3849, 2024.

Łabuz, T. A.: Environmental Impacts—Coastal Erosion and Coastline Changes. In: The BACC II Author Team (ed.): Second Assessment of Climate Change for the Baltic Sea Basin, Springer International Publishing, Cham, 381–396, https://doi.org/10.1016/10.1007/978-3-319-16006-1_20, 2015.

Łabuz, T. A.; Kowalewska-Kalkowska, H.: Coastal erosion caused by the heavy storm surge of November 2004 in the southern Baltic Sea. In: Climate Research, 48, 1, 93–101, 2011.

Lindgren, E.; Tuomi, L.; Huess, V.; Kanarik, H.: EU Copernicus Marine Service Product User Manual for Baltic Sea Wave Hindcast Product BALTICSEA_MULTI-YEAR_WAV_003_015. Issue: 2.0, Mercator Ocean International, Toulouse, 2024. https://documentation.marine.copernicus.eu/PUM/CMEMS-BAL-PUM-003-015.pdf, accessed 02.12.2024.

LKN.SH (Landesbetrieb für Küstenschutz, Nationalpark und Meeresschutz Schleswig-Holstein): Fachplan Küstenschutz Ostseeküste: Grundlagen. Einteilung in Küstenabschnitte. Abschnitt Schleimünde, Husum: LKN.SH, 2020. https://schleswig-holstein.de/mm/downloads/LKN/kuestenschutz_fachplaene/1_Ostseekueste/2_Grundlagen/2-2_Abschnitt_82_Schleimuendung.pdf, accessed 29.08.2024.

Luijendijk, A.; Hagenaars, G.; Ranasinghe, R.; Baart, F.; Donchyts, G.; Aarninkhof, S.: The State of the World's Beaches. In: Scientific Reports, 8, 1, 6641, 2018.

McFeeters, S. K.: The use of the Normalized Difference Water Index (NDWI) in the delineation of open water features. In: International Journal of Remote Sensing, 17, 7, 1425–1432, 1996.

Meier, H. E. M.; Kniebusch, M.; Dieterich, C.; Gröger, M.; Zorita, E.; Elmgren, R.; Myrberg, K.; Ahola, M. P.; Bartosova, A.; Bonsdorff, E.; Börgel, F.; Capell, R.; Carlén, I.; Carlund, T.; Carstensen, J.; Christensen, O. B.; Dierschke, V.; Frauen, C.; Frederiksen, M.; Gaget, E.; Galatius, A.; Haapala, J. J.; Halkka, A.; Hugelius, G.; Hünicke, B.; Jaagus, J.; Jüssi, M.; Käyhkö, J.; Kirchner, N.; Kjellström, E.; Kulinski, K.; Lehmann, A.; Lindström, G.; May, W.; Miller, P. A.; Mohrholz, V.; Müller-Karulis, B.; Pavón-Jordán, D.; Quante, M.; Reckermann, M.; Rutgersson, A.; Savchuk, O. P.; Stendel, M.; Tuomi, L.; Viitasalo, M.; Weisse, R.; Zhang, W.: Climate change in the Baltic Sea region: a summary. In: Earth System Dynamics, 13, 1, 457–593, 2022.

MELUND (Ministerium für Energiewende; Landwirtschaft; Umwelt; Natur und Digitalisierung): Generalplan Küstenschutz Schleswig-Holstein. Fortschreibung 2022, Kiel: MELUND, 2022. https://www.schleswig-holstein.de/DE/fachinhalte/K/kuestenschutz/Downloads/Generalplan.pdf?__blob=publicationFile&v=3, accessed 02.09.2024.

Mentaschi, L.; Vousdoukas, M. I.; Pekel, J.-F.; Voukouvalas, E.; Feyen, L.: Global long-term observations of coastal erosion and accretion. In: Scientific Reports, 8, 1, 12876, 2018.

Nicholls, R. J.; Cazenave, A.: Sea-level rise and its impact on coastal zones. In: Science (New York, N.Y.), 328, 5985, 1517–1520, 2010.

Otsu, N.: A Threshold Selection Method from Gray-Level Histograms. In: IEEE Transactions on Systems, Man, and Cybernetics, 9, 1, 62–66, 1979.

Pang, T.; Wang, X.; Nawaz, R. A.; Keefe, G.; Adekanmbi, T.: Coastal erosion and climate change: A review on coastal-change process and modeling. In: Ambio, 52, 12, 2034–2052, 2023.

Passeri, D. L.; Hagen, S. C.; Medeiros, S. C.; Bilskie, M. V.; Alizad, K.; Wang, D.: The dynamic effects of sea level rise on low-gradient coastal landscapes: A review. In: Earth's Future, 3, 6, 159–181, 2015.

Pikelj, K.; Ružić, I.; Ilić, S.; James, M. R.; Kordić, B.: Implementing an efficient beach erosion monitoring system for coastal management in Croatia. In: Ocean & Coastal Management, 156, 223–238, 2018.

Planet Labs: Planet Application Program Interface: In Space for Life on Earth, 2024. https://api.planet.com, accessed 29.08.2024.

Rad, A. M.; Kreitler, J.; Sadegh, M.: Augmented Normalized Difference Water Index for improved surface water monitoring. In: Environmental Modelling & Software, 140, 105030, 2021.

Scheffler, D.; Hollstein, A.; Diedrich, H.; Segl, K.; Hostert, P.: AROSICS: An Automated and Robust Open-Source Image Co-Registration Software for Multi-Sensor Satellite Data. In: Remote Sensing, 9, 7, 676, 2017.

Schütt, E. M.: Monitoring Coastal Change from Space. Assessing the applicability to monitor shoreline evolution with multitemporal Sentinel-2 MSI data in Schleswig-Holstein. Master thesis, Kiel University, Kiel, 2022.

Schwarzer, K.; Diesing, M.; Larson, M.; Niedermeyer, R.-O.; Schumacher, W.; Furmanczyk, K.: Coastline evolution at different time scales – examples from the Pomeranian Bight, southern Baltic Sea. In: Marine Geology, 194, 1-2, 79–101, 2003.

Senechal, N.; Ruiz de Alegría-Arzaburu, A.: Seasonal imprint on beach morphodynamics. In: Jackson, D. W.; Short, A. D. (eds.): Sandy Beach Morphodynamics, Elsevier, 461–486, https://doi.org/10.1016/10.1016/B978-0-08-102927-5.00020-5, 2020.

Siewert, M.; Schlamkow, C.; Saathoff, F.: Spatial analyses of 52 years of modelled sea state data for the Western Baltic Sea and their potential applicability for offshore and nearshore construction purposes. In: Ocean Engineering, 96, 284–294, 2015.

Smith, K. E. L.; Terrano, J. F.; Pitchford, J. L.; Archer, M. J.: Coastal Wetland Shoreline Change Monitoring: A Comparison of Shorelines from High-Resolution WorldView Satellite Imagery, Aerial Imagery, and Field Surveys. In: Remote Sensing, 13, 15, 3030, 2021.

StALU (Staatliches Amt für Umwelt und Natur): Regelwerk Küstenschutz Mecklenburg-Vorpommern: Übersichtsheft. Grundlagen, Grundsätze, Standortbestimmung und Ausblick, Rostock: StALU, 2021. https://www.stalu-mv.de/serviceassistent/download?id=1639581, accessed 29.08.2024.

Sunny, D. S.; Islam, K. A.; Mullick, M. R. A.; Ellis, J. T.: Performance study of imageries from MODIS, Landsat 8 and Sentinel-2 on measuring shoreline change at a regional scale. In: Remote Sensing Applications: Society and Environment, 28, 100816, 2022.

Thomas, N.; Pertiwi, A. P.; Traganos, D.; Lagomasino, D.; Poursanidis, D.; Moreno, S.; Fatoyinbo, L.: Space-Borne Cloud-Native Satellite-Derived Bathymetry (SDB) Models Using ICESat-2 And Sentinel-2. In: Geophysical Research Letters, 48, 6, 2021.

Tiede, J.; Jordan, C.; Moghimi, A.; Schlurmann, T.: Long-term shoreline changes at large spatial scales at the Baltic Sea: remote-sensing based assessment and potential drivers. In: Frontiers in Marine Science, 10, 2023.

Toure, S.; Diop, O.; Kpalma, K.; Maiga, A. S.: Shoreline Detection using Optical Remote Sensing: A Review. In: ISPRS International Journal of Geo-Information, 8, 2, 75, 2019.

Vitousek, S.; Buscombe, D.; Vos, K.; Barnard, P. L.; Ritchie, A. C.; Warrick, J. A.: The future of coastal monitoring through satellite remote sensing. In: Cambridge Prisms: Coastal Futures, 1, 2023.

Vos, K.; Harley, M. D.; Splinter, K. D.; Simmons, J. A.; Turner, I. L.: Sub-annual to multi-decadal shoreline variability from publicly available satellite imagery. In: Coastal Engineering, 150, 160–174, 2019.

Vos, K.; Harley, M. D.; Splinter, K. D.; Walker, A.; Turner, I. L.: Beach Slopes From Satellite-Derived Shorelines. In: Geophysical Research Letters, 47, 14, 2020.

Vousdoukas, M. I.; Ranasinghe, R.; Mentaschi, L.; Plomaritis, T. A.; Athanasiou, P.; Luijendijk, A.; Feyen, L.: Sandy coastlines under threat of erosion. In: Nature Climate Change, 10, 3, 260–263, 2020.

Wang, Z.; Liu, J.; Li, J.; Zhang, D. D.: Multi-Spectral Water Index (MuWI): A Native 10-m Multi-Spectral Water Index for Accurate Water Mapping on Sentinel-2. In: Remote Sensing, 10, 10, 1643, 2018.

Weisse, R.; Dailidienė, I.; Hünicke, B.; Kahma, K.; Madsen, K.; Omstedt, A.; Parnell, K.; Schöne, T.; Soomere, T.; Zhang, W.; Zorita, E.: Sea level dynamics and coastal erosion in the Baltic Sea region. In: Earth System Dynamics, 12, 3, 871–898, 2021.

Williams, A. T.; Rangel-Buitrago, N.; Pranzini, E.; Anfuso, G.: The management of coastal erosion. In: Ocean & Coastal Management, 156, 4–20, 2018.

Wright, L.; Short, A.: Morphodynamic variability of surf zones and beaches: A synthesis. In: Marine Geology, 56, 1-4, 93–118, 1984.

Wulder, M. A.; Loveland, T. R.; Roy, D. P.; Crawford, C. J.; Masek, J. G.; Woodcock, C. E.; Allen, R. G.; Anderson, M. C.; Belward, A. S.; Cohen, W. B.; Dwyer, J.; Erb, A.; Gao, F.; Griffiths, P.; Helder, D.; Hermosilla, T.; Hipple, J. D.; Hostert, P.; Hughes, M. J.; Huntington, J.; Johnson, D. M.; Kennedy, R.; Kilic, A.; Li, Z.; Lymburner, L.; McCorkel, J.; Pahlevan, N.; Scambos, T. A.; Schaaf, C.; Schott, J. R.; Sheng, Y.; Storey, J.; Vermote, E.; Vogelmann, J.; White, J. C.; Wynne, R. H.; Zhu, Z.: Current status of Landsat program, science, and applications. In: Remote Sensing of Environment, 225, 127–147, 2019.

xcube developers: xcube - An xarray-based EO data cube toolkit: n.d. https://xcube.readthedocs.io/en/latest/index.html, accessed 28.09.2024.

Xu, H.: Modification of normalised difference water index (NDWI) to enhance open water features in remotely sensed imagery. In: International Journal of Remote Sensing, 27, 14, 3025–3033, 2006.

Xu, N.: Detecting Coastline Change with All Available Landsat Data over 1986–2015: A Case Study for the State of Texas, USA. In: Atmosphere, 9, 3, 107, 2018.

Ziegler, B.; Heyen, A.: Rückgang der Steilufer an der schleswig-holsteinischen westlichen Ostseeküste. In: MEYNIANA, 57, 2005.